

# INVESTIGATION OF THE TURBULENT NEAR-WAKE SQUARE CYLINDER BY MEANS OF THE EMPIRICAL MODE DECOMPOSITION

**Nicolas Mazellier**

Laboratoire PRISME  
Université d'Orléans  
8 rue Léonard de Vinci  
45072 Orléans cedex 2  
France

nicolas.mazellier@univ-orleans.fr

**Stéphane Loyer**

Laboratoire PRISME  
Université d'Orléans  
8 rue Léonard de Vinci  
45072 Orléans cedex 2  
France

stephane.loyer@univ-orleans.fr

**Azeddine Kourta**

Laboratoire PRISME  
Université d'Orléans  
8 rue Léonard de Vinci  
45072 Orléans cedex 2  
France

azeddine.kourta@univ-orleans.fr

## ABSTRACT

The near-wake of a square cylinder is investigated by means of the Empirical Mode Decomposition. This processing technique is coupled to a separation criterion to extract both the coherent and the turbulent fluctuations of the experimental time series. The performance of the extraction procedure is emphasized by analysing energy spectrum and probability density functions. The statistics of the Reynolds stresses of both the coherent and turbulent fluctuations are then reported and analysed. It is found that the properties of the coherent and turbulent fluctuations differ noticeably.

## 1 Introduction

Flow around bluff body is frequently encountered in nature and engineering applications such as transport, heat exchangers for which partial or massive flow separations resulting from either pressure or curvature effects may have dramatic impact onto aerodynamic performances, structure vibration or noise production for instance. Non linearity and unsteadiness characterising turbulent separated flows (see, e.g., Kourta *et al.*, 1987) imply that standard processing technique such as Fourier transform would be irrelevant to model turbulence and its interaction with the so-called coherent structures Hussain & Reynolds (1970). To overcome that issue adapted processing techniques are required.

The so-called coherent structures have been extensively studied in literature. Hussain & Reynolds (1970) introduced the triple decomposition to take into account the specific influence of coherent structures. In conjunction with the usual Reynolds ensemble averaging, these authors used the phase averaging to emphasize the role of the coherent structures on the transport equations. The approach

introduced by Hussain & Reynolds (1970) requires thereby well defined phase reference, i.e. a single tone signal. For instance, Lyn & Rodi (1994) and Lyn *et al.* (1995) compared the ensemble averaged and phase averaged flow in the near-wake of a square cylinder. In their work, the phase reference was the output of a pressure transducer set in the side wall of the square cylinder. Recently, Perrin *et al.* (2007) investigated the near-wake of a circular cylinder equipped with a pressure sensor as phase reference. They found that phase jitter between the reference phase and the flow may lead to significant discrepancies. To address this issue, these authors used the POD coefficients of the first two modes as a local phase reference.

Huang *et al.* (1998) introduced the so-called Empirical Mode Decomposition (referred to as EMD in the following) to analyse signals recorded from non linear and/or non stationary physical process. This processing technique was then extensively used in physics, biology or medicine. EMD was recently applied to turbulence to investigate internal intermittency (Huang *et al.*, 2008) and forced turbulence (Foucher & Ravier, 2010). Mazellier & Foucher (2011) used the EMD algorithm to investigate synthetic periodic flapping superimposed to turbulent fluctuations and introduced an objective criterion to discriminate between flapping and turbulent fluctuations. In this paper, we aim at extending that approach to the investigation of the turbulent near wake of a square cylinder.

The paper is organised as follows. The experimental set-up is detailed in section 2. Then the basics of the EMD algorithm and the separation criterion are briefly explained in section 3. Finally, the analysis of the near-wake cylinder by means of EMD is reported in section 4.

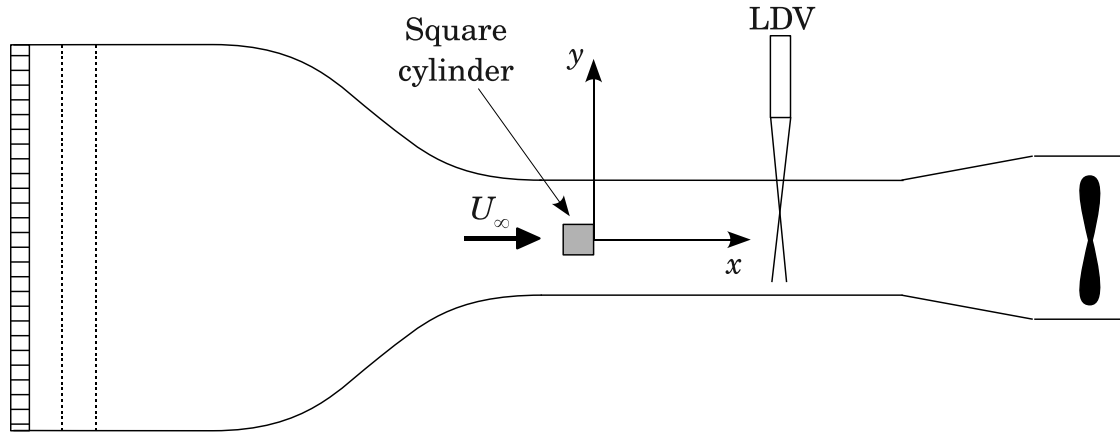


Figure 1. Schematic of the experimental facility.

## 2 Experimental set-up

Experiments have been carried out in an open-loop wind tunnel with a 2 m long and 50 cm wide square test section where the free-stream turbulence level is as low as 0.4%. A square cylinder of  $H = 60$  mm side spanning the tunnel width is set close to the test section inlet. The Reynolds number  $Re = U_\infty H / \nu$  (where  $U_\infty$  and  $\nu$  stand for the free-stream velocity and the kinematic viscosity, respectively) is  $4 \times 10^4$  in this study. A schematic of the experimental set-up is depicted in Fig. 1. The origin of the coordinate system  $(x, y)$  coincides with the centre of the square cylinder base.

The velocity field in the near wake of the square cylinder is investigated by means of two-components (514.5nm, 488nm) Laser Doppler Velocimetry (LDV) system with a 6W Argon-Ion laser (Spectra-Physics, Stabillite 2017) as light source. The flow seeding is ensured by saturating the wind tunnel room with olive oil droplets ( $\sim 1\mu\text{m}$  in diameter) generated by a particle seeding apparatus. The LDV probe was mounted on a 3D traversing system controlled by a computer and data were collected in the backward mode and processed with a BSA processor (Dantec) set in a non-coincident single measurement per burst mode. Velocity measurements were performed in the mid-plane of the working section.

Both streamwise ( $x$ -axis) and transverse ( $y$ -axis) velocity components (referred to as  $u$  and  $v$ , respectively) were collected at various locations in the near-wake of the square cylinder. In this paper, we report only results obtained at  $x/H = 1$ . For each measurement station, several parameters such as the photomultiplier intensity and/or the window filtering were adjusted to optimize the mean data rate. Regarding the investigated region of the flow, the sampling rate was ranging from 2kHz to 20kHz resulting in time-series lasting between 50s (in the wake of the cylinder) and 5s (in the free stream), respectively. These values were high enough to resolve the large scale flow dynamics. The LDA technique is known to produce non-equidistant time samples avoiding consequently a direct spectral analysis (Fourier transform). To overcome this drawback, a linear interpolation method was used to recover uniformly sampled data in order to investigate the large scale dynamics of the flow since this procedure only alters the high frequency range.

## 3 The Empirical Mode Decomposition

### 3.1 The basics

The Empirical Mode Decomposition (EMD) is a data-driven processing technique introduced by Huang *et al.* (1998) which has been designed to analyse non stationary and non linear physics. Actually, it has been designed in support to the Hilbert transform to properly define the instantaneous frequency of a time series. The combination of both EMD and Hilbert transform is also designated as Hilbert-Huang Transform Huang *et al.* (1998).

EMD is based on the decomposition of a time series  $s(t)$  as follows

$$s(t) = d(t) + r(t), \quad (1)$$

where  $d(t)$  and  $r(t)$  are high (*detail*) and low (*trend*) frequency components, respectively. The low frequency component  $r(t)$  is estimated as the local mean of the upper and the lower envelopes of  $s(t)$ . Once this low frequency component  $r(t)$  is extracted it is used as a new signal onto which the EMD algorithm can be applied and so on until no more oscillation can be detected. Accordingly, the original signal  $s(t)$  can be expressed as follows

$$s(t) = \sum_{m=1}^N \text{IMF}_m + r_N, \quad (2)$$

where  $\text{IMF}_m$  is the  $m^{\text{th}}$  Intrinsic Mode Function (i.e. the low frequency component of the  $(m-1)^{\text{th}}$  Intrinsic Mode Function) and  $r_N$  is the final residual. A sifting procedure developed by Huang *et al.* 1998 ensures two conditions to be fulfilled:

- i) the total number of zero crossings and extremes of each IMF differ by one at most,
- ii) the local mean value defined as the average between the lower and the upper envelopes of each IMF is zero.

Given that the EMD is by definition a data-driven technique, therefore locally self-adaptive, two important remarks have to be made to emphasize the main differences between EMD and standard approaches:

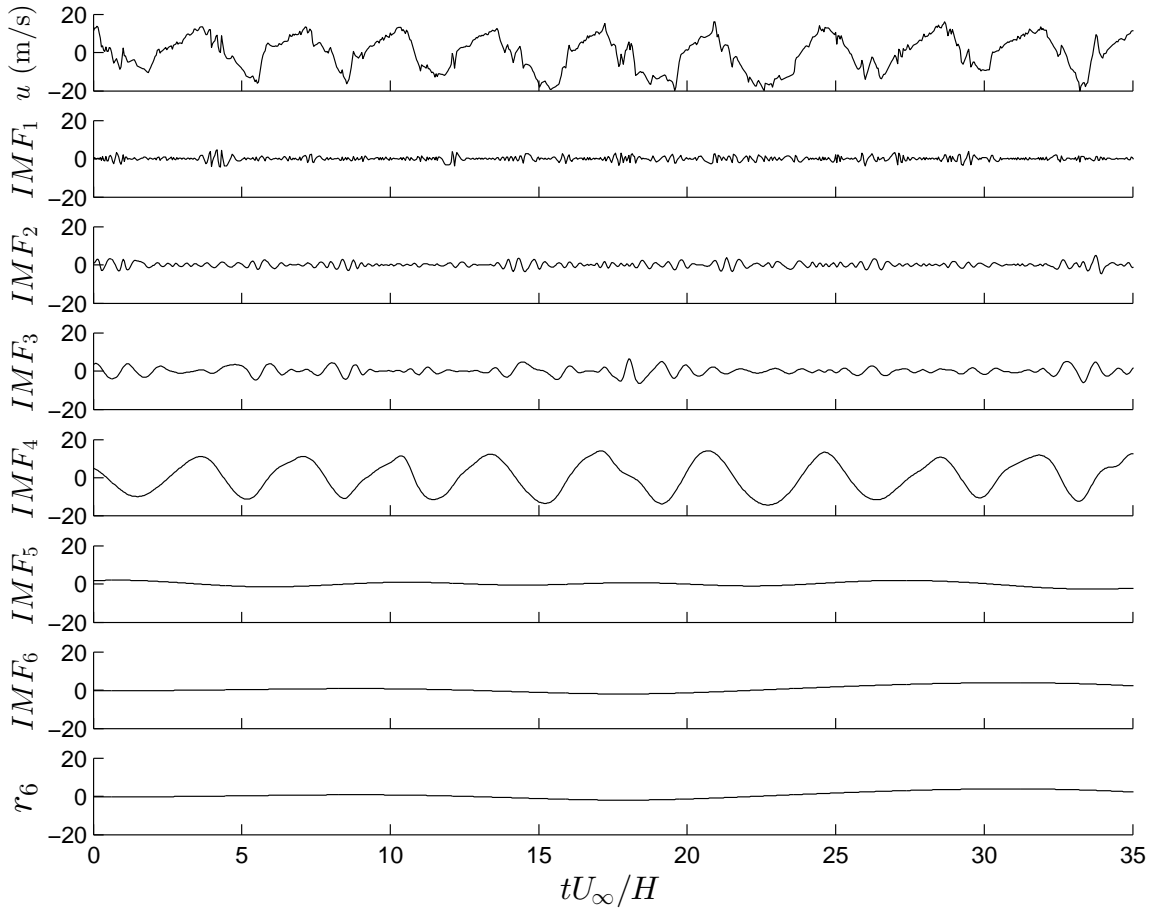


Figure 2. Typical decomposition of a velocity time-series by means of EMD. The original signal is displayed in the top plot.

- i) the shape of the IMFs is not assumed *a priori* unlike the Fourier transform.
- ii) the extraction of the IMFs is not conditioned by a statistical convergence.

### 3.2 The mode separation

A typical EMD decomposition of a velocity time series  $u(t)$  collected at  $x/H = 1$  and  $y/H = 0.6$  is shown in Fig. 2. The raw signal  $u(t)$  (top plot in Fig. 2) is characterized by both low and high frequency fluctuations which are related to vortex shedding and turbulence, respectively. A comparison between  $u(t)$  and the modes extracted by EMD clearly shows that the low frequency signature, i.e. the vortex shedding, is mostly concentrated in  $IMF_4$  for this particular example.

The results displayed in Fig. 2 seem to indicate that the raw signal  $u(t)$  is the combination of a coherent contribution  $\tilde{u}(t)$  and a turbulent one  $u'(t)$  similarly to the so-called triple decomposition :

$$u(t) = \tilde{u}(t) + u'(t). \quad (3)$$

The main advantage of the EMD algorithm stands in the fact that the formulation of the coherent part does not rely on a reference phase unlike phase averaging technique.

The arising issue stands in the definition of a criterion to discriminate between the IMFs pertaining the coherent part and those contributing to the turbulent part. Re-

cent studies have been devoted to the definition of such a criterion (Flandrin *et al.*, 2004; Foucher & Ravier, 2010; Mazellier & Foucher, 2011). In this work, we combine the EMD algorithm to the "ressemblance" criterion introduced by Mazellier & Foucher (2011) which consists in reconstructing the signal from the high frequency to the low frequency modes according to Eq. (2). At each step, the value of the maximum cross-correlation between two successively reconstructed signals is used to define a cut-off mode  $m_c$  separating coherent and turbulent parts. Mazellier & Foucher (2011) evaluated the performance of that method on synthetic signals built from the combination of velocity signals recorded in homogeneous and isotropic turbulence and low frequency single tone or chirp. They reported successful results even though they showed that the large-scale of the reconstructed turbulent signal was altered by the so-called mode mixing issue ((see Rilling & Flandrin, 2008)). To address this issue, we have applied a modified version of the EMD algorithm recently introduced by Segalen *et al.* (2011) which is based on a modulation-demodulation step to minimize the mode mixing during the extraction of the IMFs.

The performance of the separation between coherent and turbulent fluctuations is emphasized by the spectral analysis plotted in Fig. 3 which compares the energy spectrum computed from  $u(t)$  recorded at  $x/H = 1$  and  $y/H = 0.6$  (top plot in 2) and from its turbulent contribution  $u'(t)$  extracted from the procedure described above. The vortex shedding frequency is clearly identified on the energy spectrum of  $u(t)$  by an intense peak occurring at Strouhal num-

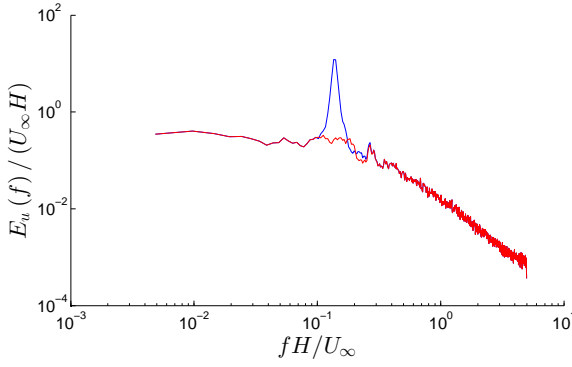


Figure 3. Dimensionless energy spectra computed from the raw  $u(t)$ , blue line) and its inferred turbulent contribution  $u'(t)$ , red line) at  $x/H = 1$  and  $y/H = 0.6$ .

ber  $fH/U_\infty \approx 0.14$ . The energy spectrum computed from  $u'(t)$  does not exhibit such a peak which illustrates the potential interest of EMD to separate both coherent (vortex shedding) and turbulent fluctuations.

#### 4 Statistics in the near-wake

The procedure detailed in the previous section was extended to the measurements collected in the near-wake of the square cylinder. At each measurement location, the EMD algorithm was coupled to the separation criterion to study both streamwise ( $u$ ) and transverse ( $v$ ) velocity components recorded by the LDV system. This procedure enables to extract both coherent (i.e.,  $\tilde{u}$  and  $\tilde{v}$ ) and turbulent (i.e.,  $u'$  and  $v'$ ) fluctuations onto which usual statistical tools might be applied.

The profile of the dimensionless turbulent kinetic energy  $k/U_\infty^2$  (where  $k = (2\langle u'^2 \rangle + \langle v'^2 \rangle)/2$  assuming axisymmetry around  $y$  according to the results reported by Norberg (1998)) computed from the raw signal is plotted in Fig. 4. This variable is compared to the turbulent kinetic energy  $k'/U_\infty^2$  and the coherent kinetic energy  $\tilde{k}/U_\infty^2$  which are calculated from the turbulent and coherent contributions extracted from the EMD algorithm. The results displayed in Fig. 4 evidence that the energy contained in the coherent part of the signal is about twice that contained in the turbulent part. One can notice also that  $k'/U_\infty^2$  becomes negligible beyond  $y/H = 1.5$  which coincides with the location where the velocity profile becomes flat.

The dimensionless normal stresses computed from the raw, coherent and turbulent velocity fluctuations are plotted in Figs. 5 and 6 for the streamwise and transverse components, respectively. For both components, one can see clearly see that the pattern of the normal stresses computed from the coherent fluctuations follows closely that of the raw signal. Indeed,  $\langle \tilde{u}^2 \rangle$  which is null in the potential region rises up until it reaches a maximum at  $y/H \approx 0.6$ . This location coincides with the mixing layer at the wake boundary. Besides,  $\langle \tilde{v}^2 \rangle$  peaks at the center of the wake. Furthermore, the amplitude of the normal stresses computed from the coherent fluctuations is of the order of that computed from the raw signal. The intensities of the normal stresses computed from the turbulent fluctuations are much smaller than those of the coherent fluctuations especially for the transverse component. Moreover, in the region located between the center of the wake and the mixing layer, the normal stresses computed from the turbulent fluctuations

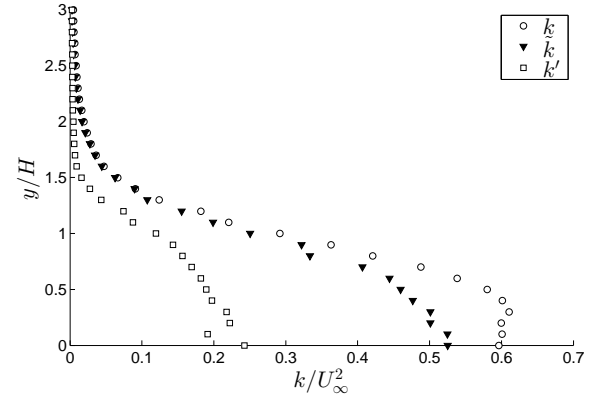


Figure 4. transverse profile of the dimensionless turbulent kinetic energy at  $x/H = 1$ .

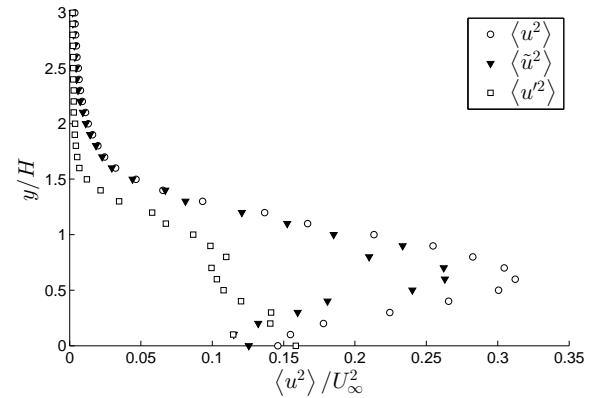


Figure 5. transverse profile of the dimensionless streamwise normal stress at  $x/H = 1$ .

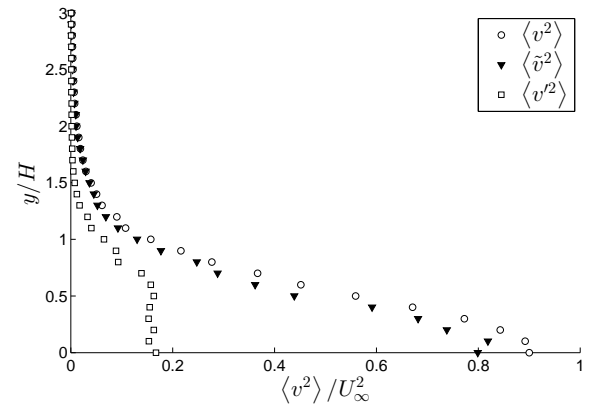


Figure 6. transverse profile of the dimensionless transverse normal stress at  $x/H = 1$ .

are nearly homogeneous and isotropic unlike the normal stresses computed from the coherent fluctuations.

The probability density function  $\mathcal{P}$  of the original signal  $u(t)$  and the inferred turbulent fluctuations  $u'(t)$  are compared in Fig. 7. This plot evidences that the statistical properties of  $u$  and  $u'$  differ noticeably. Indeed, while the  $\mathcal{P}(u)$  is characterised by a bi-modal shape reflecting the influence of the periodic vortex shedding,  $\mathcal{P}(u')$  tends to the normal distribution (dotted line in Fig. 7).

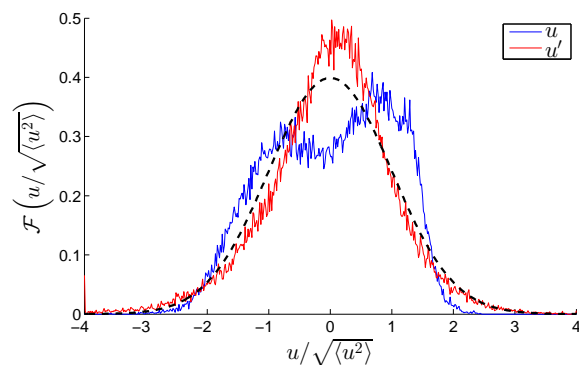


Figure 7. Probability density function of the streamwise velocity component.

## 5 Conclusion

The near-wake of a square cylinder has been experimentally investigated by means of the Empirical Mode Decomposition. This technique coupled with an appropriate separation criterion aims at discriminating between the coherent and turbulent contributions of the raw signal. The spectral analysis has emphasized that the EMD algorithm succeeded in separating both contributions. The statistics of the near-wake cylinder has been reported through second order moments. It has been showed that the turbulent contribution is much smaller than the coherent one. Furthermore, the turbulence is found nearly homogeneous and isotropic. Finally, the statistic analysis has been completed by the study of the probability density functions which tend to gaussian distribution for the turbulent component.

## REFERENCES

- Flandrin, P, Rilling, G & Goncalvés, P 2004 Empirical mode decomposition as a filter bank. *IEEE Signal Proc Lett* **11**, 112–114.
- Foucher, F & Ravier, P 2010 Determination of turbulence properties by using empirical mode decomposition on periodic and random perturbed flows. *Exp Fluids* **49**, 379–390.
- Huang, N. E., Shen, Z., Long, S. R., Wu, W. C., Shih, H. H., Zheng, Q., Yen, N. C., Tung, C. C. & Liu, H. H. 1998 The empirical mode decomposition and the hilbert spectrum for nonlinear and non-stationary time series analysis. *Proc. R. Soc. Lond. A* **454**, 903–995.
- Huang, Y. X., Schmitt, F. G., Lu, Z. M. & L., Liu Y. 2008 An amplitude-frequency study of turbulent scaling intermittency using empirical mode decomposition and hilbert spectral analysis. *Europhys Lett* **84**, 40010.
- Hussain, A. K. M. F. & Reynolds, W. C. 1970 The mechanics of an organized wave in turbulent shear flow. *J Fluid Mech* **41**, 241–258.
- Kourta, A., Boisson, H. C., Chassaing, P. & Minh, H. Ha 1987 Nonlinear interaction and the transition to turbulence in the wake of a circular cylinder. *Journal of Fluid Mechanics* **181**, 141–161.
- Lyn, D. A., Einav, S., Rodi, W. & Park, J.-H. 1995 A laser-doppler velocimetry study of ensemble-averaged characteristics of the turbulent near wake of a square cylinder. *Journal of Fluid Mechanics* **304**, 285–319.
- Lyn, D. A. & Rodi, W. 1994 The flapping shear layer formed by flow separation from the forward corner of a square cylinder. *Journal of Fluid Mechanics* **267**, 353–376.
- Mazellier, N. & Foucher, F. 2011 Separation between coherent and turbulent fluctuations: what can we learn from the empirical mode decomposition? *Experiments in Fluids* **51** (2), 527–541.
- Norberg, C. 1998 Ldv-measurements in the near-wake of a circular cylinder. In *Advances in Understanding of Bluff Body Wakes and Vortex-Induced Vibration*.
- Perrin, R., Braza, M., Cid, E., Cazin, S., Barthet, A., Sevrain, A., Mockett, C. & Thiele, F. 2007 Obtaining phase averaged turbulence properties in the near wake of a circular cylinder at high reynolds number using pod. *Experiments in Fluids* **43** (2-3), 341–355.
- Rilling, G. & Flandrin, P. 2008 One or two frequencies? the empirical mode decomposition answers. *IEEE Trans on Signal Proc* **56**, 85–95.
- Segalen, C., Jabloun, M., Ravier, P., Harba, R., Ledee, R. & Nguyen, L. D. 2011 On the separation of heart sound components using a translated empirical mode decomposition. In *Proceedings of the 4th International Symposium on Applied Sciences in Biomedical and Communication Technologies*.